The Journal of Infectious Diseases

MAJOR ARTICLE

An Experimental Human Blood-Stage Model for Studying *Plasmodium malariae* Infection

John Woodford,[1,2] Katharine A. Collins,[1,a] Anand Odedra,[1] Claire Wang,[3] Ihn Kyung Jang,[4] Gonzalo J. Domingo,[4] Rebecca Watts,[1] Louise Marquart,[1] Matthew Berriman,[5] Thomas D. Otto,[5,6] and James S. McCarthy[1,2]

[1]QIMR Berghofer Medical Research Institute, [2]The University of Queensland, and [3]Queensland Paediatric Infectious Diseases Laboratory, Brisbane, Australia; [4]PATH, Seattle, Washington; and [5]Wellcome Sanger Institute, Hinxton, and [6]Centre of Immunobiology, Institute of Infection, Immunity, and Inflammation, College of Medical, Veterinary, and Life Sciences, University of Glasgow, Glasgow, United Kingdom

(See the Editorial Commentary by Sutherland, on pages 864–6.)

Background. *Plasmodium malariae* is considered a minor malaria parasite, although its global disease burden is underappreciated. The aim of this study was to develop an induced blood-stage malaria (IBSM) model of *P. malariae* to study parasite biology, diagnostic assays, and treatment.

Methods. This clinical trial involved 2 healthy subjects who were intravenously inoculated with cryopreserved *P. malariae*–infected erythrocytes. Subjects were treated with artemether-lumefantrine after development of clinical symptoms. Prior to antimalarial therapy, mosquito-feeding assays were performed to investigate transmission, and blood samples were collected for rapid diagnostic testing and parasite transcription profiling. Serial blood samples were collected for biomarker analysis.

Results. Both subjects experienced symptoms and signs typical of early malaria. Parasitemia was detected 7 days after inoculation, and parasite concentrations increased until antimalarial treatment was initiated 25 and 21 days after inoculation for subjects 1 and 2 respectively (peak parasitemia levels, 174 182 and 50 291 parasites/mL, respectively). The parasite clearance half-life following artemether-lumefantrine treatment was 6.7 hours. Mosquito transmission was observed for 1 subject, while in vivo parasite transcription and biomarkers were successfully profiled.

Conclusions. An IBSM model of *P. malariae* has been successfully developed and may be used to study the biology of, diagnostic testing for, and treatment of this neglected malaria species.

Clinical Trials Registration. ACTRN12617000048381.

Keywords. *Plasmodium malariae*; induced blood-stage malaria; transmission; diagnostics; transcriptomics; biomarkers; CHMI; pLDH.

Recent global malaria control efforts have appropriately focused on the most virulent *Plasmodium* species infecting humans, *Plasmodium falciparum*, with lesser efforts on the second most important species, *Plasmodium vivax*. However, the effort to eradicate malaria necessitates an understanding of all infective species. In comparison to *P. falciparum* and *P. vivax*, our understanding of *Plasmodium malariae* biology and pathogenesis is very limited. While the majority of malaria morbidity and mortality is associated with *P. falciparum* and *P. vivax*, *P. malariae* as a coinfecting pathogen is found in 4%–24% of cases and has a wide geographical distribution [1–3]. *P. malariae* can cause prolonged and often subpatent infection [4] and chronic renal dysfunction [5], and it may modulate the clinical course and transmission of other species [6]. Recent sequencing studies of a *P. malariae* draft genome [7] and establishment of a good quality reference genome [8] heralds a much greater understanding of this neglected tropical pathogen. However, many questions remain about the biology of this species, the efficacy of current control measures, the dynamics of transmission, the performance of routine diagnostic testing [9, 10], and the efficacy of standard antimalarial treatments [11–13].

Volunteer infection study (VIS) clinical trials represent a powerful approach to assess the efficacy of malaria vaccines and antimalarial drugs [14–16]. VIS trials allow for detailed evaluation of parasite growth kinetics, pharmacodynamics of the antimalarial activity of candidate drugs, and parasite transmission to vector mosquitoes. They also provide an opportunity to evaluate parasite biology and characterize host immunological responses in a controlled environment. Data from such studies can provide

Received 21 December 2018; editorial decision 1 February 2019; accepted 6 March 2019; published online March 11, 2019.

[a]Current affiliation: Department of Medical Microbiology, Radboud University Medical Center, Nijmegen, the Netherlands.

Presented in part: Australian Society for Infectious Diseases Annual Scientific Meeting, Gold Coast, Australia, 10–12 May 2018.

Correspondence: J. Woodford, MBBS, QIMR Berghofer Medical Research Institute, 300 Herston Rd, Herston QLD 4006, Australia (john.woodford@uqconnect.edu.au).

The Journal of Infectious Diseases® 2020;221:948–55

DOI: 10.1093/infdis/jiz102

information for the development of diagnostic tests, vaccines, and drugs. While reliable VIS models have been developed for *P. falciparum* and *P. vivax*, none have been developed for *P. malariae*. The aim of this study was to develop an induced blood-stage malaria model (IBSM) with a wild isolate of *P. malariae*.

METHODS

Study Design

This was a clinical trial involving 2 sequential cohorts of 1 subject each (clinical trials registration ACTRN12617000048381). The study was approved by the QIMR Berghofer Medical Research Institute Human Research Ethics Committee and conducted in accordance with the Declaration of Helsinki. Subjects provided written informed consent prior to participation in the study. The primary objective was to determine the safety and infectivity of the *P. malariae* isolate in healthy subjects following inoculation with blood-stage parasites. The secondary objectives were to define parasite growth curves and clearance profiles after administration of the antimalarial drug artemether-lumefantrine and to investigate the infectivity of parasites to vector mosquitoes. The exploratory objectives were to evaluate the in vivo pattern of gene transcription of *P. malariae*, to establish host and parasite biomarker dynamics during early stage infection, and to evaluate a commercially available rapid diagnostic test (in cohort 2 only).

Study Subjects

Healthy adults aged 18–55 years were eligible for participation. Subjects were required to be malaria naive, blood group A or AB, and Rh(D) positive. A full list of the inclusion/exclusion criteria for this study is included in the Supplementary Materials.

P. malariae Inoculum

The *P. malariae* isolate (HMPBS-*Pm*) used in this study was derived from blood donated by a traveler returning from Guinea, Africa, who presented to the Royal Brisbane and Women's Hospital with symptomatic, polymerase chain reaction (PCR)–confirmed *P. malariae* infection. The genome of this isolate has been sequenced and has previously been compared to the *P. malariae* reference genome [8]. The production of parasite inoculum banks from donor blood specimens has been previously described for *P. falciparum* and *P. vivax* [17, 18].

Study Procedures

After intravenous injection of parasites on study day 0, subjects were monitored by daily telephone calls for the first 5 days. From day 6 onward, subjects visited the study site daily for clinical monitoring of adverse events (AEs), signs and symptoms of malaria parasite infection, and blood sampling for measurement of the parasitemia level.

Antimalarial treatment with artemether-lumefantrine was instituted following development of clinical symptoms consistent with malaria parasite infection or if the parasitemia level exceeded 200 000 parasites/mL, a safety threshold based on previous IBSM studies [19]. Prior to treatment, mosquito feeding assays were performed, and blood samples were collected for transcriptomic analysis, biomarker studies, and rapid diagnostic tests. Treatment consisted of 6 doses (administered 12 hours apart) of artemether-lumefantrine (Riamet, Novartis Pharmaceuticals Australia). Safety assessments and blood sampling to monitor the parasitemia level were conducted twice daily until parasite clearance and then at protocol-specified visits until 3 months after treatment, to monitor for any signs of recrudescence.

Safety and Parasitemia Assessment

Safety monitoring of subjects included recording adverse events, measuring vital signs, physical examination, electrocardiography (ECG), and measuring clinical laboratory parameters (via hematologic studies; clinical chemistry analyses, including creatinine studies; and urinalysis, including urinary protein studies).

The parasitemia level was measured using quantitative PCR targeting the gene encoding *P. malariae* 18S ribosomal RNA (rRNA), as previously described [17]. Search of the *P. malariae* genome confirmed that this *Plasmodium* species carries 2 copies of this gene target.

Calculation of Parasite Reduction Ratio (PRR)

The PRR and corresponding parasite clearance half-life were estimated using the slope of the optimal fit for the log-linear relationship of the decay in parasitemia level following artemether-lumefantrine treatment, as previously described [20].

Mosquito Feeding Assays

Transmission of gametocytes to *Anopheles stephensi* mosquitoes was evaluated using a direct skin feeding assay (DFA) and a direct membrane feeding assay (DMFA) as previously described for *P. falciparum* [21]. Mosquito midguts were dissected and tested for transmission positivity, using light microscopy with mercurochrome staining and also using quantitative PCR targeting the gene encoding *P. malariae* 18S rRNA.

Biomarker Dynamics Assessment

P. falciparum histidine-rich protein 2 (HRP2), pan-genus lactate dehydrogenase (LDH), *P. vivax* LDH, and human C-reactive protein (CRP) were quantified in blood samples collected at various time points, using the recently developed Q-plex array enzyme-linked immunosorbent assay kit (Quansys Biosciences, Logan, UT) [22]. Untransformed quantitative parasitemia and quantitative biomarker measurements were correlated using a Spearman correlation.

Assessment of Rapid Diagnostic Testing

Rapid diagnostic testing was performed using the lateral flow antigen detection test CareStart Malaria HRP-2/pLDH (Pf/pan) Combo Test (Apacor, Berkshire, United Kingdom). Blood specimens collected at the peak parasitemia level prior to treatment were tested as per manufacturer guidelines.

Assessment of *P. malariae* Transcription Profile

A 20-mL blood sample collected at the peak parasitemia level prior to treatment was depleted of leukocytes by using a Plasmodipur push column, and infected erythrocytes were concentrated using a Percoll gradient [23]. RNA was extracted and complementary DNA synthesized using a SMART-seq2 kit (Clonetech/Takara) with 32 cycles of amplification and PhiX bacteriophage as a control. The library was sequenced on a MiSeq (150-bp reads) and a HiSeq 2500 Illumina machine (125-bp paired-end reads). Sequence reads from the subject were excluded by alignment against the *H. sapiens* HS19 reference genome, using BWA as part of an automatic pipeline at the Wellcome Sanger Institute. Parasite messenger RNA reads were mapped against the *P. malariae* reference genome PmUG01 [8] from geneDB.org, using STAR default settings [24]. Visualization was performed in BamView [25] after transforming the read file into the BAM format by using SAMtools [26]. *P. malariae* reads were compared to existing *P. falciparum* data to describe the pattern of gene transcription and determine the developmental stage of parasites. Correlation to the *P. falciparum* data set [27, 28] from PlasmoDB was performed in R, using the corrgram function. To enable the comparison, 1:1 orthologs between *P. falciparum* and *P. malariae* were determined by orthoMCL [29]. To better assess the more variable subtelomeric gene families, the genomic reads of the inoculum isolate HMPBS-*Pm* (accession ERS567899) were assembled using MaSuRCA (default parameters) [30]. Genome annotation was performed with Companion [31], using *P. malariae* UG01 as a reference (parameter Augustus ab initio set to 0.2).

RESULTS

Subjects

A total of 8 subjects were screened for eligibility, and 2 subjects were enrolled in the study (1 in each cohort). Subject 1 and subject 2 were healthy white men aged 24 and 18 years, respectively.

Safety

A total of 35 AEs were reported (Table 1), the majority of which (30 of 35 [85.7%]) were attributed to *P. malariae* infection. The remaining AEs were either attributed to direct skin feeding with mosquitoes (2 of 35) or considered to be unrelated to study procedures (3 of 35). Most AEs (27 of 35 [77.2%]) were mild in severity, with the remaining AEs moderate in severity. None of the AEs reported in this study were classified as serious. Both subjects experienced chills, fatigue, headache, malaise, myalgia, and nausea during the study. Fever and transient moderate neutropenia were also recorded for both subjects and were consistent with malaria parasite infection.

Parasitemia

Parasitemia was first detected 7 days after inoculation, and the level increased at a similar rate in both subjects until antimalarial treatment was initiated 25 and 21 days after inoculation for subject 1 and subject 2, respectively (Figure 1). Parasitemia levels at the time of treatment were 140 890 and 50 291 parasites/mL, respectively. Clearance of parasitemia occurred following artemether-lumefantrine treatment in both subjects, with no recrudescence observed up to 3 months after treatment. Furthermore, there was no evidence of persisting gametocytemia, as would be indicated by persistent detection of *P. malariae* DNA. The peak parasitemia level recorded for subject 1 was 174 182 parasites/mL, which occurred 4 hours after treatment. The parasitemia level at the time of treatment was the highest level recorded for

Table 1. Adverse Events Recorded for Each Subject

	Events, No.	
Adverse Event	Subject 1	Subject 2
Abdominal discomfort	0	2
Arthralgia	1	0
Chills	1	1
Cough	0	1
Decreased appetite	0	1
Dizziness	1	0
Fatigue	1	2
Furuncle	0	1
Headache	1	4
Influenza-like illness	1	0
Malaise	1	1
Myalgia	2	1
Nausea	1	2
Neutrophil count decrease	1	1
Puncture site induration	1	1
Pyrexia	1	3
Upper respiratory tract infection	0	1
Total	13	22

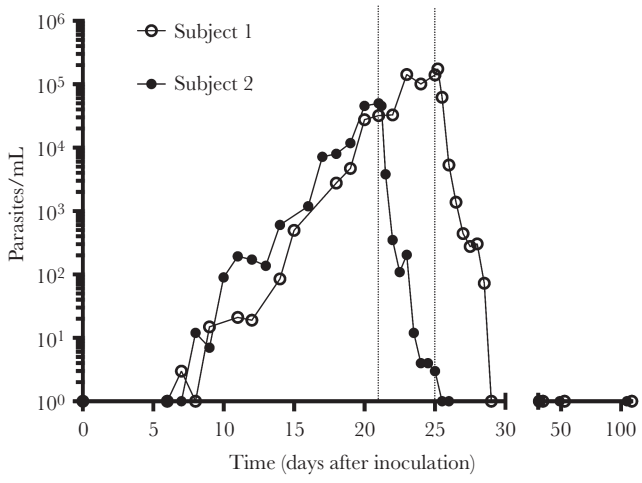

Figure 1. Parasitemia profile for each subject. Vertical dotted lines indicate the day that treatment with artemether-lumefantrine was initiated (day 25 for subject 1 and day 21 for subject 2).

subject 2. The overall PRR was 143.4 (95% confidence interval [CI], 73.7–278.7), and the parasite clearance half-life was 6.70 hours (95% CI, 5.91–7.74). Parasite clearance occurred at a similar rate in each subject.

Transmission to Mosquitoes

DFAs and DMFAs were performed just prior to antimalarial treatment (25 and 21 days after inoculation for subject 1 and subject 2 respectively). The average feeding rate of mosquitoes was high (minimum, 95.1%), and the mortality rate was <26% for all assays (Supplementary Table 1). Transmission of parasites to mosquitoes was detected for subject 1, with 1 of 34 mosquitoes (2.9%) becoming infected following the DFA. Light microscopy confirmed that the infected mosquito contained a single oocyst. No transmission was observed with the DFA for subject 2 or with the DMFA for either subject.

Biomarker Dynamics and Rapid Diagnostic Testing

Serial blood sampling for evaluation of biomarkers of malaria parasite infection was performed for subject 2. Quantitative analyses revealed that HRP2 and *P. vivax* pLDH remained undetectable throughout the course of parasitemia. Pan-genus pLDH first became detectable on day 13 after inoculation, at a parasitemia level of 137 parasites/mL (Figure 2). The pan-genus pLDH level was strongly correlated with the parasitemia level (R = 0.78; 95% CI, .52–.91), although there was an evident time lag in biomarker response. CRP levels increased with parasitemia levels, although the relationship was weaker (R = 0.13; 95% CI, −.32–.53; Figure 2). The time lag in biomarker response was more pronounced for CRP; peak values occurred 36 hours after initiation of treatment, and values remained elevated after parasite clearance. A CareStart Malaria HRP-2/pLDH (Pf/pan) rapid diagnostic test performed on day 21 after inoculation, at a parasitemia level of 50 291 parasites/mL, had a negative result.

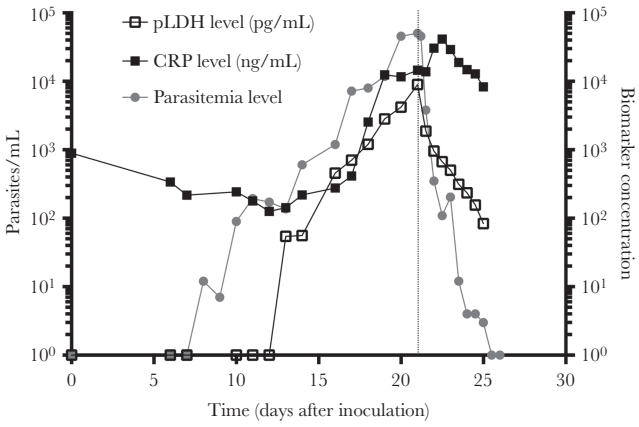

Figure 2. Biomarker results for subject 2. The vertical dotted line indicates the day that treatment with artemether-lumefantrine was initiated (ie, day 21). CRP, C-reactive protein; pLDH, parasite lactate dehydrogenase.

Transcriptome Analysis

A blood specimen collected from subject 1 at the time of the peak pretreatment parasitemia level (140 890 parasites/mL) underwent RNA sequencing (RNA-Seq). Extraction of the RNA generated 100 ng to 3.3 µg of total complementary DNA for high-throughput sequencing. The raw reads can be found under the sample accession number ERS1699009. The accession numbers of the sequencing reads for the Illumina MiSeq and HiSeq 2500 are ERX2597961 and ERR2690580, respectively.

A large proportion of sequenced reads corresponded to the host (51.2%), which were excluded automatically by the Wellcome Sanger Institute sequencing pipeline, or to the PhiX control (25.6%); 5.8% of sequenced reads were mapped against *P. malariae*. Of these, approximately 75% corresponded to rRNA. While the mRNA yield of *P. malariae* was low (1.45%), deep sequencing (>260 million reads) enabled approximately 3.8 million informative parasite-derived reads to be obtained that clearly mapped to the *P. malariae* genome. This represents a theoretical coverage of 33 times all coding sequences. If normalized coverage (in reads per kilobase of transcript, per million reads mapped [RPKM]) detection thresholds of 5 or 10 are assumed, expression was detected for 948–1463 genes (Figure 3).

The RPKM raw reads count per gene for the 15 genes with highest expression are shown in Supplementary Table 2. Two of these (PmUG01_14016600 and PmUG01_14018200) encode gamete antigen 27/25. The *P. malariae* genome includes 20 apparently intact copies of this gene, compared with a single copy in other examined *Plasmodium* species [8]. Of these 20 copies, only 3 were highly expressed, with comparatively low expression in others (Figure 4).

Parasite development stages within the sample were determined by comparing gene expression profiles against 2 time-course data sets from *P. falciparum* (Supplementary Figure 1). Correlations were low (0.12–0.37) but peaked against the 32-hour intraerythrocytic form (0.35) and gametocyte II (0.37).

The structure of expressed genes could be clearly resolved by visual inspection in which mRNA reads were compared to PmUG01 reference genome predictions (Figure 3A). Expression signals with peaks in the 5′ untranslated region (UTR) or 5′ intergenic regions were seen in coverage for several highly expressed genes (Figure 3B–D). In some cases, discrete coverage distal to an existing gene prediction was indicative of a novel noncoding RNA (Figure 3B). In other cases, the 5′ UTR coverage bias appeared to reflect overamplification during library production (Figure 3C). No evidence of a long UTR or novel noncoding RNA was found in the regions of higher expression when comparing the *P. malariae* genome PmUG01_05020900 to published data sets on PlasmoDB for *P. falciparum* orthologs (PF3D7_0825100; Figure 3D). RNA-Seq data were also used to correct the intron-exon structure of predicted genes in the current annotation of the reference genome (Figure 3E). It was possible to perform an exploratory analysis of expression of predicted exported proteins

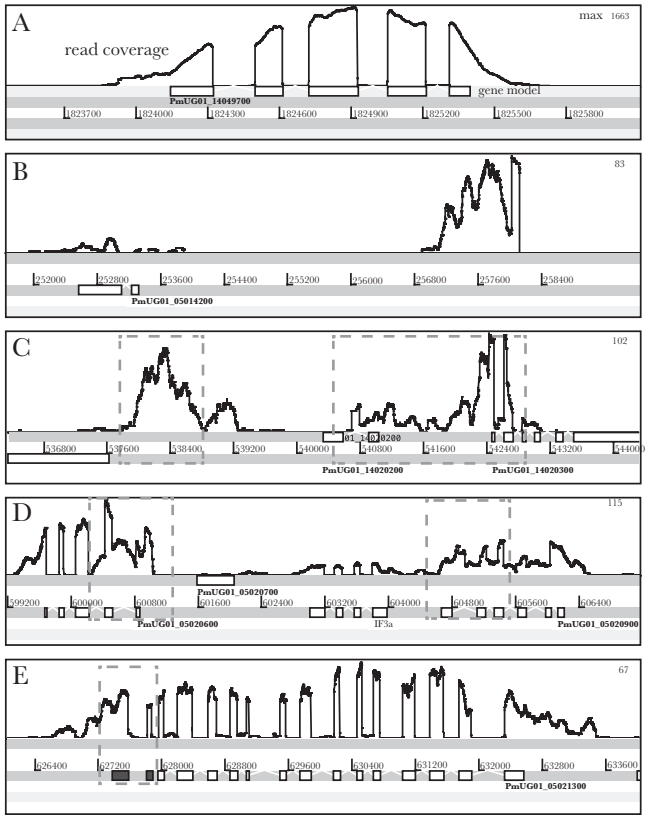

Figure 3. Examples of read coverage determined by RNA sequencing analysis. The coverage plot represents the number of reads mapped over each base, plotted in black. RNA reads are mapped to the reference genome (long light gray rows; numbers indicate the position on the chromosome). White and dark gray bars represent predicted exons. Coverage without a predicted exon may represent an untranslated region (UTR), noncoding RNA (ncRNA), or missing exons in the reference genome. Read depth represents a guide to the degree of expression. *A*, Example of good gene coverage, with clear exon-intron boundaries and no mapped reads between exons (white bars). Coverage left and right are from UTRs. *B*, Example of a gene with low expression (left side; white bars) and expression approximately 4 kb downstream of putative ncRNA. *C*, Example of potential 5′UTR amplification as compared to the rest of the gene (dashed boxes). *D*, Example of overlapping expression (dashed boxes). The exon-intron boundaries are not clear, and expression appears to be in between exons of 1 gene. This may be due to an overlapping UTR of the neighbor gene or ncRNA on the reverse strand. *E*, Example of gene correction with the help of RNA sequencing analysis. Two new exons (dark gray bars in dashed box) can be added to the existing 13 predicted exons (white bars) within the reference genome.

that may contribute to parasite virulence. The *P. malariae* genome published by Rutledge et al [8] reported 2 new tandemly organized multigene families (*fam-l* and *fam-m*) that share structural similarity with a *P. falciparum* merozoite surface protein, encoded by Rh5 (PF3D7_0424100), that is essential for erythrocyte invasion. We were unable to find evidence for expression of any *fam-l* and *fam-m* pairs, even when RNA-Seq data were matched to an assembled and annotated genome from the study isolate. In contrast, evidence of expression (RPKM, >10) was found for other subtelomeric gene family members, of which 22 encoded putatively exported proteins, including 8 PHIST proteins and 1 STP1. Ten *pir* genes also appeared to be expressed, but all had a RPKM value of < 5, based on the PmGN01 annotation.

DISCUSSION

Inoculation of healthy subjects with the *P. malariae* HMPBS-Pm clinical isolate resulted in a safe and reproducible course of parasitemia that was well tolerated. Specifically, there was no evidence of renal impairment or late recurrent infection in the 3 months following treatment. The overall nature, frequency, and severity of AEs was similar to that reported following experimental inoculation with blood stages of other *Plasmodium* species, where mild-to-moderate symptoms attributable to malaria were observed with increasing parasitemia levels [17, 18]. Significantly, no AEs were classified as severe or serious, and no biochemical abnormalities were noted.

Parasite growth following inoculation was slower for *P. malariae*, compared with that reported for *P. falciparum* or *P. vivax* [17, 18], consistent with the slower 72-hour intraerythrocytic life cycle and smaller number of merozoite schizogony per cycle characteristic of the species [32]. The pyrogenic threshold of *P. malariae* infection in this study was lower than that reported for historical case series from the malariotherapy era, where the median parasitemia at first fever was reported to range from 997 800 to 2 664 000 parasites/mL [19]. This may be due to differences in interindividual infection tolerability, the strain of *P. malariae*, or increased subject monitoring in modern clinical trials.

Parasite clearance following administration of artemether-lumefantrine was slower than that estimated for species with a shorter 48-hour intraerythrocytic life cycle. The parasite clearance half-life following artemether-lumefantrine treatment was 6.7 hours (95% CI, 5.91–7.74) in this study. As a comparison, a parasite clearance half-life of >5.0 hours is used to indicate artemisinin resistance in *P. falciparum* [33]. Nonetheless, standard-dose artemether-lumefantrine was effective, without evidence of recrudescence at follow-up 3 months after treatment. However, there are reports of treatment failure in the literature [9, 13]. Postulated mechanisms of a refractory response of *P. malariae* infection to artemether-lumefantrine include a relative reduction in drug exposure due to a prolonged parasite life cycle or delayed hepatic schizogony, parasite dormancy and reduced susceptibility to treatment, an undescribed hypnozoite stage, and genetic subpopulations with intrinsic drug resistance [11, 34]. Treatment success in this study may be related to a relatively low parasitemia level at the time of treatment or to the susceptibility of this *P. malariae* strain. In the absence of a hepatic stage of infection in the IBSM model, it is not possible to assess the effect of delayed hepatic schizogony or as-yet-undescribed hypnozoite forms.

The successful transmission of *P. malariae* to mosquitoes confirms gametocytogenesis in the model. While only a single transmission episode occurred, the low rate of transmission is consistent with that for other *Plasmodium* species at low levels of parasitemia/gametocytemia and validates the model as a tool for the evaluation of parasite transmission [21]. Relatively little is known regarding the dynamics of *P. malariae* gametocyte

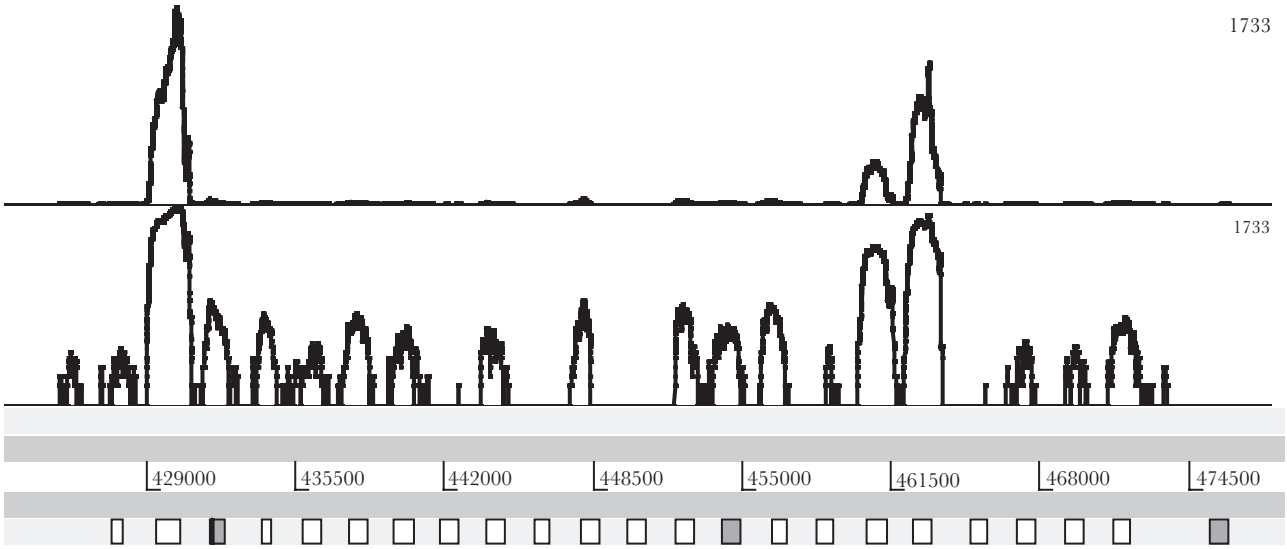

Figure 4. Expression of gamete antigen 27/25 (PmG27/25). Artemis view of the PmG27/25 locus. The boxes show the 22 PmG27/25 gene copies (white bars) and 2 pseudogenes (gray bars). The top plot is raw coverage showing high-level expression of 3 gene copies, and the bottom plot is log-transformed coverage showing lower-level expression of the other copies.

commitment and transmission [19]. Significantly, *P. malariae* coinfection has been implicated in enhanced *P. falciparum* gametocytogenesis, suggesting that this species could potentiate transmission of more-virulent disease [35–37]. Such interactions are exceedingly difficult to confirm in the field, making this model attractive to characterizing parasite biology and developing transmission-blocking interventions.

Pan-genus pLDH was the only *Plasmodium*-specific biomarker detected during the course of *P. malariae* infection, and its levels were positively correlated with parasitemia levels. Results of rapid diagnostic testing targeting pan-genus pLDH were, however, negative, despite the presence of symptoms consistent with malaria for 72 hours prior to testing. This is consistent with previous reports of poor assay performance and an approximately 30% detection rate [10, 38, 39]. Although pan-genus pLDH appears to have the appropriate characteristics for a screening test, with a proportional increase with the parasitemia level and a relatively prompt clearance after treatment, the lack of sensitive rapid diagnostic testing for this *Plasmodium* species represents a challenge to case detection, true estimates of disease burden, and elimination efforts. An increased CRP level with an increasing parasitemia level reflects a nonspecific host response but is consistent with the correlation between this biomarker and disease severity in other *Plasmodium* species [40]. *P. malariae* infection in our study demonstrated different biomarker dynamics to those described in *P. falciparum* infection, with a relatively delayed lag period in pLDH positivity after the first observation of parasitemia, as well as a more pronounced CRP signal [22]. While a larger sample is required to confirm these findings, such interspecies differences highlight the need for potentially different methods of detection. The high-throughput loop-mediated isothermal amplification assay has been demonstrated to be an effective and sensitive alternative detection method for other neglected *Plasmodium* species not readily identified by current rapid diagnostic tests, although application in *P. malariae* cases is limited, and field applications may be limited by cost [41].

Although exploratory assessment of the *P. malariae* transcription profile in vivo isolated only a limited amount of mRNA for analysis, this proof of concept offers a number of prospects for further study of parasite biology and enabled the reference genome annotation for *P. malariae* to be refined. We did not find evidence of expression among the *pir* genes, which have been shown to have a major role in virulence in some other species [42, 43], or among the novel transmembrane protein families (*fam-m* or *fam-l*). Instead, other exported proteins, including PHISTs, were identified, suggesting these proteins may play a more prominent role in this species. Serial assessment of parasite transcription during the course of infection would also be informative and indicate whether antigenic variation or adhesion molecule upregulation are parasite strategies permitting the prolonged, latent infections that have been previously described [4]. The identification of putative gametocyte gene transcripts may enable the development of a targeted reverse transcription PCR probe for more-sensitive analysis of gametocyte dynamics, as has been developed for both *P. falciparum* and *P. vivax* [44].

In conclusion, we have outlined an experimental system of *P. malariae* infection that offers the potential to study this neglected tropical pathogen and subsequently accelerate the development of diagnostic tests, drugs, and vaccines. The logistic challenges and financial costs of field-efficacy studies are even greater for *P. malariae* than for the more virulent malaria parasite

species, owing to relatively lower case numbers, challenges in case identification, and the relative frequency of coinfection. Nonetheless, the global effort to eradicate malaria necessitates an understanding of all infective species. The ability to undertake experimental study of *P. malariae* malaria in a dedicated clinical trial setting represents a significant resource, enhancing safety and enabling the design and conduct of well-controlled research.

Supplementary Data

Supplementary materials are available at *The Journal of Infectious Diseases* online. Consisting of data provided by the authors to benefit the reader, the posted materials are not copyedited and are the sole responsibility of the authors, so questions or comments should be addressed to the corresponding author.

Notes

Acknowledgements. We thank Dennis Shanks, for serving as the medical monitor; Mandy Sanders, for coordinating the sequencing; Adam Potter, for assistance with manuscript preparation; the index patient, for contributing the inoculum bank; the staff of Q-Pharm, for coordinating the study; and the subjects in this study.

Financial support. This work was supported by the National Health and Medical Research Council (Practitioner Fellowship [to J. S. M.] and Program Grant 1132975), the Government of Queensland (Health Research Fellowship to J. S. M.), and the Bill and Melinda Gates Foundation (grant to G. J. D.).

Potential conflicts of interest. All authors: No reported conflicts of interest. The authors have submitted the ICMJE Form for Disclosure of Potential Conflicts of Interest. Conflicts that the editors consider relevant to the content of the manuscript have been disclosed.

References

1. Proietti C, Pettinato DD, Kanoi BN, et al. Continuing intense malaria transmission in northern Uganda. Am J Trop Med Hyg **2011**; 84:830–7.
2. Zhou M, Liu Q, Wongsrichanalai C, et al. High prevalence of *Plasmodium malariae* and *Plasmodium ovale* in malaria patients along the Thai-Myanmar border, as revealed by acridine orange staining and PCR-based diagnoses. Trop Med Int Health **1998**; 3:304–12.
3. Lo E, Nguyen K, Nguyen J, et al. Plasmodium malariae prevalence and csp gene diversity, Kenya, 2014 and 2015. Emerg Infect Dis **2017**; 23:601–10.
4. Vinetz JM, Li J, McCutchan TF, Kaslow DC. Plasmodium malariae infection in an asymptomatic 74-year-old Greek woman with splenomegaly. N Engl J Med **1998**; 338:367–71.
5. Gilles HM, Hendrickse RG. Nephrosis in Nigerian children. Role of *Plasmodium malariae*, and effect of antimalarial treatment. Br Med J **1963**; 2:27–31.
6. Mueller I, Zimmerman PA, Reeder JC. *Plasmodium malariae* and *Plasmodium ovale*–the "bashful" malaria parasites. Trends Parasitol **2007**; 23:278–83.
7. Ansari HR, Templeton TJ, Subudhi AK, et al. Genome-scale comparison of expanded gene families in *Plasmodium ovale* wallikeri and *Plasmodium ovale* curtisi with *Plasmodium malariae* and with other Plasmodium species. Int J Parasitol **2016**; 46:685–96.
8. Rutledge GG, Böhme U, Sanders M, et al. *Plasmodium malariae* and *P. ovale* genomes provide insights into malaria parasite evolution. Nature **2017**; 542:101–4.
9. Betson M, Sousa-Figueiredo JC, Atuhaire A, et al. Detection of persistent Plasmodium spp. infections in Ugandan children after artemether-lumefantrine treatment. Parasitology **2014**; 141:1880–90.
10. Grobusch MP, Hänscheid T, Zoller T, Jelinek T, Burchard GD. Rapid immunochromatographic malarial antigen detection unreliable for detecting *Plasmodium malariae* and *Plasmodium ovale*. Eur J Clin Microbiol Infect Dis **2002**; 21:818–20.
11. Rutledge GG, Marr I, Huang GKL, et al. Genomic characterization of recrudescent *Plasmodium malariae* after treatment with artemether/lumefantrine. Emerg Infect Dis **2017**; 23:1300–7.
12. Visser BJ, Wieten RW, Kroon D, et al. Efficacy and safety of artemisinin combination therapy (ACT) for non-falciparum malaria: a systematic review. Malar J **2014**; 13:463.
13. Dinko B, Oguike MC, Larbi JA, Bousema T, Sutherland CJ. Persistent detection of *Plasmodium falciparum*, *P. malariae*, *P.* ovale curtisi and *P.* ovale wallikeri after ACT treatment of asymptomatic Ghanaian school-children. Int J Parasitol Drugs Drug Resist **2013**; 3:45–50.
14. Sauerwein RW, Roestenberg M, Moorthy VS. Experimental human challenge infections can accelerate clinical malaria vaccine development. Nat Rev Immunol **2011**; 11:57–64.
15. Kamau E, Alemayehu S, Feghali KC, et al. Measurement of parasitological data by quantitative real-time PCR from controlled human malaria infection trials at the Walter Reed Army Institute of Research. Malar J **2014**; 13:288.
16. McCall MB, Netea MG, Hermsen CC, et al. Plasmodium falciparum infection causes proinflammatory priming of human TLR responses. J Immunol **2007**; 179:162–71.
17. McCarthy JS, Griffin PM, Sekuloski S, et al. Experimentally induced blood-stage *Plasmodium vivax* infection in healthy volunteers. J Infect Dis **2013**; 208:1688–94.
18. McCarthy JS, Sekuloski S, Griffin PM, et al. A pilot randomised trial of induced blood-stage *Plasmodium falciparum* infections in healthy volunteers for testing efficacy of new antimalarial drugs. PLoS One **2011**; 6:e21914.
19. McKenzie FE, Jeffery GM, Collins WE. *Plasmodium malariae* blood-stage dynamics. J Parasitol **2001**; 87:626–37.
20. Marquart L, Baker M, O'Rourke P, McCarthy JS. Evaluating the pharmacodynamic effect of antimalarial drugs in

clinical trials by quantitative PCR. Antimicrob Agents Chemother **2015**; 59:4249–59.
21. Collins KA, Wang CY, Adams M, et al. A controlled human malaria infection model enabling evaluation of transmission-blocking interventions. J Clin Invest **2018**; 128:1551–62.
22. Jang IK, Tyler A, Lyman C, Kahn M, Kalnoky M, Rek JC, et al. Simultaneous quantification of Plasmodium antigens and host factor C-reactive protein in asymptomatic individuals with confirmed malaria by use of a novel multiplex immunoassay. J Clin Microbiol **2019**; 57:e00948–18.
23. Rivadeneira EM, Wasserman M, Espinal CT. Separation and concentration of schizonts of *Plasmodium falciparum* by Percoll gradients. J Protozool **1983**; 30:367–70.
24. Dobin A, Davis CA, Schlesinger F, et al. STAR: ultrafast universal RNA-seq aligner. Bioinformatics **2013**; 29:15–21.
25. Carver T, Harris SR, Otto TD, Berriman M, Parkhill J, McQuillan JA. BamView: visualizing and interpretation of next-generation sequencing read alignments. Brief Bioinform **2013**; 14:203–12.
26. Li H, Handsaker B, Wysoker A, et al.; 1000 Genome Project Data Processing Subgroup. The sequence alignment/map format and SAMtools. Bioinformatics **2009**; 25:2078–9.
27. López-Barragán MJ, Lemieux J, Quiñones M, et al. Directional gene expression and antisense transcripts in sexual and asexual stages of *Plasmodium falciparum*. BMC Genomics **2011**; 12:587.
28. Otto TD, Wilinski D, Assefa S, et al. New insights into the blood-stage transcriptome of *Plasmodium falciparum* using RNA-Seq. Mol Microbiol **2010**; 76:12–24.
29. Li L, Stoeckert CJ Jr, Roos DS. OrthoMCL: identification of ortholog groups for eukaryotic genomes. Genome Res **2003**; 13:2178–89.
30. Zimin AV, Marçais G, Puiu D, Roberts M, Salzberg SL, Yorke JA. The MaSuRCA genome assembler. Bioinformatics **2013**; 29:2669–77.
31. Steinbiss S, Silva-Franco F, Brunk B, et al. Companion: a web server for annotation and analysis of parasite genomes. Nucleic Acids Res **2016**; 44:W29–34.
32. Collins WE, Jeffery GM. Plasmodium malariae: parasite and disease. Clin Microbiol Rev **2007**; 20:579–92.
33. Ashley EA, Dhorda M, Fairhurst RM, et al.; Tracking Resistance to Artemisinin Collaboration (TRAC). Spread of artemisinin resistance in Plasmodium falciparum malaria. N Engl J Med **2014**; 371:411–23.
34. Markus MB. Dormancy in mammalian malaria. Trends Parasitol **2012**; 28:39–45.
35. McKenzie FE, Jeffery GM, Collins WE. Plasmodium malariae infection boosts *Plasmodium falciparum* gametocyte production. Am J Trop Med Hyg **2002**; 67:411–4.
36. Gnémé A, Guelbéogo WM, Riehle MM, et al. Plasmodium species occurrence, temporal distribution and interaction in a child-aged population in rural Burkina Faso. Malar J **2013**; 12:67.
37. Bousema JT, Drakeley CJ, Mens PF, et al. Increased *Plasmodium falciparum* gametocyte production in mixed infections with *P. malariae*. Am J Trop Med Hyg **2008**; 78:442–8.
38. Heutmekers M, Gillet P, Maltha J, et al. Evaluation of the rapid diagnostic test CareStart pLDH Malaria (Pf-pLDH/pan-pLDH) for the diagnosis of malaria in a reference setting. Malar J **2012**; 11:204.
39. Maltha J, Gillet P, Bottieau E, Cnops L, van Esbroeck M, Jacobs J. Evaluation of a rapid diagnostic test (CareStart Malaria HRP-2/pLDH (Pf/pan) Combo Test) for the diagnosis of malaria in a reference setting. Malar J **2010**; 9:171.
40. Paul R, Sinha PK, Bhattacharya R, Banerjee AK, Raychaudhuri P, Mondal J. Study of C reactive protein as a prognostic marker in malaria from Eastern India. Adv Biomed Res **2012**; 1:41.
41. Britton S, Cheng Q, Grigg MJ, William T, Anstey NM, McCarthy JS. A sensitive, colorimetric, high-throughput loop-mediated isothermal amplification assay for the detection of *Plasmodium knowlesi*. Am J Trop Med Hyg **2016**; 95:120–2.
42. Spence PJ, Jarra W, Lévy P, et al. Vector transmission regulates immune control of *Plasmodium virulence*. Nature **2013**; 498:228–31.
43. Brugat T, Reid AJ, Lin J, et al. Antibody-independent mechanisms regulate the establishment of chronic Plasmodium infection. Nat Microbiol **2017**; 2:16276.
44. Wampfler R, Mwingira F, Javati S, et al. Strategies for detection of Plasmodium species gametocytes. PLoS One **2013**; 8:e76316.